

1-1-2009

Rapid reduction of copper sulfide (Cu₂S) with elemental Fe and Mg using electrical discharge assisted meachanical milling (EDAMM)

Andrzej Calka
University of Wollongong, acalka@uow.edu.au

David Wexler
University of Wollongong, david_wexler@uow.edu.au

Brian J. Monaghan
University of Wollongong, monaghan@uow.edu.au

A Mosbah
University of Wollongong

P Balaz
Slovak Academy of Sciences, Slovakia

Follow this and additional works at: <https://ro.uow.edu.au/engpapers>

 Part of the [Engineering Commons](#)

<https://ro.uow.edu.au/engpapers/1244>

Recommended Citation

Calka, Andrzej; Wexler, David; Monaghan, Brian J.; Mosbah, A; and Balaz, P: Rapid reduction of copper sulfide (Cu₂S) with elemental Fe and Mg using electrical discharge assisted meachanical milling (EDAMM) 2009, 492-496.
<https://ro.uow.edu.au/engpapers/1244>

Abstract

The electric discharge assisted mechanochemical milling technique has been applied to the reduction of copper sulphide using either elemental magnesium or elemental iron as the reducing agent. X-ray diffraction was employed for phase identification of starting materials and reaction products. After only 5 min processing using the Electric discharge assisted mechanical milling (EDAMM) method, $\text{Cu}_2\text{S} + \text{Mg}$ can be fully reduced to $\text{Cu} + \text{MgS}$ with small amount of CuO , and $\text{Cu}_2\text{S} + \text{Fe}$ can be partially reduced to $\text{Cu} + \text{Cu}_5\text{FeS}_4$ (bornite). Secondary electron imaging combined with X-ray mapping was used to investigate the distribution of elements within the processed powder particles. In the case of the Mg reduced sample the product comprised large Cu grains of purity >98%, surrounded by regions of agglomerated, small particles of Cu and MgS. In the case of the Fe partially reduced sample the product comprised a mixture of Cu plus Fe phases, frequently surrounded by regions containing the bornite phase.

The morphological evidence of the existence of deformed and some re-melted particles was consistent with arguments that high local temperatures can be achieved during EDAMM processing. However the SEM results also indicated that the primary reduction reaction mechanism involved the formation of agglomerates of small particles that did not exhibit melting. Further experiments under impulse plasma mode, both with and without conventional milling applied, demonstrated that a critical condition for the reduction reactions to occur is not based on temperature alone, but on how long the particles are processed within the in the gap between the milling rod and the base, under what may be described as Dusty Plasma conditions.

Keywords: Mechanochemical synthesis; Electrochemical reactions; Solid state reactions; Reduction reactions

Article Outline

1. [Introduction](#)
 2. [Experimental](#)
 3. [Results and discussion](#)
 - 3.1. [Cu₂S–Fe](#)
 - 3.2. [Cu₂S–Mg](#)
 4. [Conclusions](#)
- [References](#)

1. Introduction

Advanced materials manufacturing methods for the future are required to be clean, non-polluting, high speed and precision processes; producing highly reliable final products. Many materials are traditionally synthesized by slow chemical reaction processes that require capital and labour intensive facilities, and are both energy and time consuming. In the present world there is strong demand for the development of modern materials and materials processing methods that could offer rapid reaction rates, high energy efficiencies, and be environmentally safe. Electric discharge assisted mechanical milling (EDAMM) is a new and exciting materials processing technique which combines the attributes of conventional mechanical milling with a range of new effects associated with electric discharges [1] and [2]. EDAMM involves mechanical milling and simultaneous application of an electrical discharge during processing of powder particles; one of the most important factors of this process being the formation of a dusty plasma environment between the powder particles which leads to formation of ions and free radicals. In addition, the powder particles are constantly being mixed and fractured by the vibrating electrode. All these factors contribute to reactivity enhancement and have the potential to drive the replacement reactions at conditions which are either not possible or require vigorous conditions in conventional processing routes. In this work, we study the application of EDAMM to generate replacement reactions on a laboratory scale. We have taken as a model reaction the displacement of Cu from Cu_2S by metals belonging to higher positions in the electrochemical series; in the case of this investigation, Mg and Fe. The mechanism of chemical reactions between powder particles surfaces induced by an electric discharge is complex and poorly understood. It is therefore an additional aim of this work to present experimental results that shed light on factors related to EDAMM that induce chemical reactions.

2. Experimental

Cu_2S powders were mixed with Fe and Mg in proportions required in order to obtain stoichiometrically the complete reduction of Cu_2S to $\text{Cu} + \text{FeS}_2$ or $\text{Cu} + \text{MgS}$, respectively. These starting powder mixtures were first mechanically pre-mixed in a conventional ball mill for 1 h under a high purity argon atmosphere. This pre-mixture was then subjected to 5 min of electric discharge assisted ball milling (EDAMM). Electric discharge assisted milling was performed in a modified vibrational laboratory rod mill. The mill was designed to produce a milling mode combining a repeated impact of a curved rod end on powder particles, placed on a vibrating hemispherical container under electrical conditions of pulsed discharges (Fig. 1). During milling, pulsed discharges are initiated at the tip of the rod and travel through the milling atmosphere and powders before terminating in the base at the centre of the hemispherical milling cell. The power supply unit is custom built specifically for discharge milling (Manufacturer: Dora Power Supplies). Radio frequency impulses are generated with voltages in the kV range and currents in the mA range. During vibration, the electric circuit is broken by small gaps between the stainless steel rod and the milling chamber base. This results in the generation of pulsed electric discharges which travel across this gap and complete the electric circuit. All milling experiments were carried out in a high purity Ar atmosphere. XRD analysis of the as-milled powders was performed using a Phillips PW1730 diffractometer with a graphite monochromator and Cu K α radiation. Phase identification was carried out using the International Centre for Diffraction Data (JCPDS-ICDD 2000) powder diffraction files

(PDF). The morphology of the powders was investigated by scanning electron microscopy (SEM) using either a Joel 7001 FEG SEM with Bruker energy dispersive X-ray spectroscopy (EDS) and X-ray mapping system, or a Leica 440 Stereoscan SEM with Oxford Instruments EDS and mapping system. Internal machine standards and internal ZAF corrections were used for EDS semi-quantitative estimates of local chemistry.

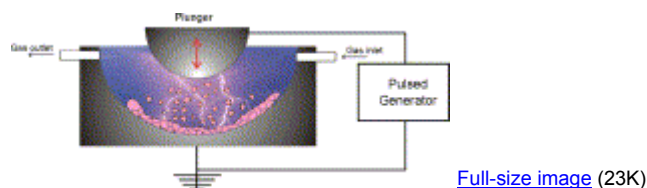


Fig. 1. Schematic of electrical discharge milling (EDAMM).

3. Results and discussion

3.1. Cu₂S–Fe

X-ray diffraction of the pre-mixed Cu₂S (chalcosine) and Fe powders, and the same mixture given a 5 min EDAMM treatment are shown in Fig. 2. After 1 h of pre-mixing in conventional ball mill there was no reaction detected between the Cu₂S and the Fe (Fig. 2a). After 5 min of EDAMM reaction of Cu₂S with elemental iron occurred and the following products were identified by XRD: pure Cu, the bornite phase (Cu₅FeS₄) and some unreacted iron (Fig. 2b, sample EDAMM processed in Ar for 5 min). SEM examination of the EDAMM milling product (Fig. 3) confirmed this result, with backscattered imaging combined with EDS spot analysis revealing Cu and Fe rich regions, of light colour in backscattered images, and finer regions containing CuFeS compound, appearing grey in backscattered images. Spot EDS analysis provided information about the three different chemistries; near pure Cu (>98%), rich near pure Fe (>98%Fe), and regions of CuFeS consistent with atomic proportions of 5Cu:1Fe:4S (Fig. 3a). Powder particle morphologies comprised a mixture of deformed particles (Fig. 3a and c) and, what appeared to be, remelted composite particles (Fig. 3b) indicating that high local temperatures were achieved during EDAMM processing. X-ray mapping (Fig. 3d–f) confirmed that the Cu-rich and Fe rich regions were separate, while the regions of CuFeS phase were fairly uniformly distributed, and often covering the outside of the Cu reduction product. In a previous paper [3] on this subject, where a mechanochemical approach has been applied the only products were elemental copper and cubic FeS (JCPDS 23-1123). This form of FeS was converted into hexagonal FeS (JCPDS 75-0602) by higher energy input. The mechanochemical reaction proceeds according to Eq. (1).

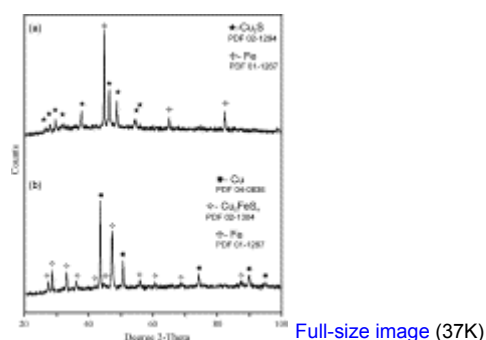
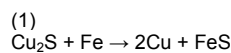
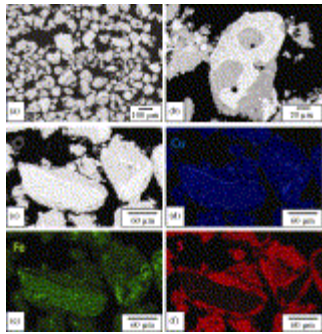


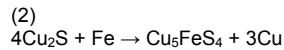
Fig. 2. XRD patterns of (a) Cu₂S + Fe starting powder after pre-mixing and (b) Cu₅FeS₄ + Cu + Fe powder produced by EDAMM.



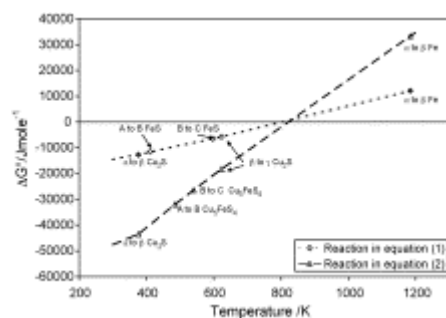
Full-size image (155K)

Fig. 3. SEM results obtained from the Cu_2S plus Fe sample discharge milled for 5 min in Ar, (a)–(c) backscattered images showing atomic number contrast, (d)–(f), X-ray maps of region (c) obtained using Cu, Fe and Cu peaks, respectively.

However, also other reaction products have been identified, e.g., bornite, hexagonal FeS and Fe_{1-x}S [4]. By milling of elemental iron with sulphur, FeS was identified in paper [5]. Bornite has also been observed [6], where high energy milling of elemental copper and pyrite was performed. There are a number of reactions that can be considered to represent bornite formation but as the starting powders in the experimental set up were Cu_2S and Fe, Eq. (2) has been chosen to represent bornite formation.



This reaction is also consistent with elemental Cu found after reaction and given in Fig. 4. Why should bornite and not FeS as reported by other researchers [1], be the predominant sulphur bearing phase after reaction? A possible answer to this question could be found by considering the equilibrium Gibb's free energy (ΔG°) of reaction for Eqs. (1) and (2). In order to assess the relative stability of these reactions a series of equilibrium ΔG° calculations was carried out for the reactions over the temperature range 298–1200 K and plotted in Fig. 4. Thermodynamic data for Cu_2S are from Kubaschewski et al. [7], data for Fe are from Lee [8] and Barin et al. [9] and data for Cu, FeS and Cu_5FeS_4 are from Barin et al. [9]. It has been assumed that thermodynamic data for $\gamma\text{-Cu}_2\text{S}$ are valid at temperatures greater than 1000 K. From Fig. 4 it can be seen that at temperatures greater than approximately 800 K the reaction given in Eq. (1) has a lower ΔG° than that of Eq. (2). The converse is true for temperatures less than approximately 800 K. Further at approximately 800 K, the ΔG° for both reactions changes from negative to positive. This indicates that above this temperature the reactions given in Eq. (1) or (2) are not spontaneous and their reaction products are not favoured. That is at above 800 K the reactions are unlikely to proceed from left to right. At temperatures less than approximately 800 K and on the assumption that Eqs. (1) and (2) represent the only possible reaction products it would be expected that Cu_5FeS_4 formation would be favoured over FeS formation at temperatures less than 800 K. This result would be consistent with a moderate and not a high temperature operating in the EDAMM chamber during the reaction.



Full-size image (33K)

Fig. 4. Gibb's free energy (ΔG°) calculations for reactions given in Eqs. (1) and (2) over the temperature range 298–1200 K. The data points represent phase changes of the reagents.

3.2. Cu_2S –Mg

Fig. 5 shows XRD results obtained from the mixture of Cu_2S and Mg. Pre-mixing for 1 h does not result in any reaction between the Cu_2S and Mg (Fig. 3a), however, after 5 min EDAMM, XRD indicates complete reaction to Cu + MgS (Fig. 3b) with additional XRD peaks indicating the presence of some CuO. The low intensity of these peaks indicate small fraction of

CuO phase in the final product. The reaction of Mg with Cu₂S to form MgS is consistent with what would be expected from a simple Ellingham diagram [12] approach to understand the thermodynamics of the reaction in Eq. (3)

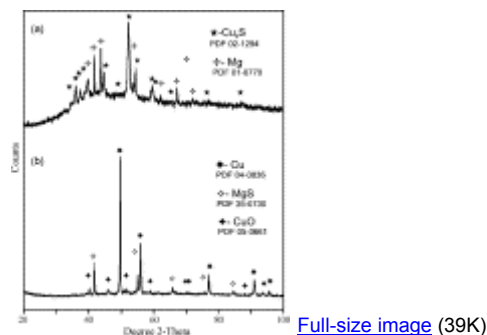
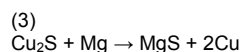


Fig. 5. XRD patterns of (a) Cu₂S + Mg starting powder after pre-mixing, and (b) MgS + Cu powder produced by EDAMM.

Using this approach the reaction would have a negative ΔG° for all temperatures that could be considered. There are only data for up to 1200 °C for the Cu₂S in this data set. This negative ΔG° would indicate that the MgS would be stable and the reaction as written would proceed from left to right.

Fig. 6 shows an SEM micrograph and X-ray mapping of Cu₂S and Mg powder after EDAMM. The example EDAMM reactions described above show one common feature – a very high reaction rate that can be achieved by significant enhancement of the thermodynamic driving force throughout generation of active species, free radicals and ions.

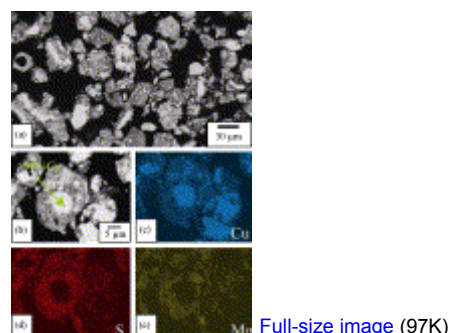


Fig. 6. SEM results obtained from the Cu₂S sample discharge milled for 5 min in Ar, (a) large area backscattered image. Cu rich regions appear white. (b) Backscattered image of particle agglomerate with Cu-rich core (>98%Cu, 50%Mg, 30%S, 0.2%Fe – mill contamination); (c)–(e) are corresponding X-ray maps for Cu, S and Mg, respectively.

In our method mechanical milling is assisted by electrical discharges. It might be expected that localized heating in our device generates high temperature plasma, and that the precursor powders are vaporized and then rapidly quenched throughout the condensation process. However, SEM results suggest a different reaction mechanism. Only in Fig. 3a very few round, melted particles can be identified, all other SEM micrographs showed agglomerates of small particles that did not exhibit melting. Although, some powder particles can be melted during EDAMM, the purpose of using the impulse mode is to prevent massive melting, and to keep the precursor powders in solid form from the beginning up to the end of the process. This leads to the formation of what we have termed a “dusty cloud” between the electrodes. The dust particles become suspended in the plasma in a region between the plunger and the mill base. The general aim is to create dusty plasma environment [10] and [11] which, we believe, will be more effective in generation of reduction reactions than thermal plasma. In the milling device used in this study, the plunger and the base vibrate independently. The purpose of vibrating the base is to ensure the powder does not lie stationary on the plunger base. If the base was not vibrating, the powder would stay at the bottom of the reaction chamber and would not be suspended between the base and the plunger. In that case the powder laying on the base is subjected to both mixing (or milling) by the plunger and discharges in the gaps between the plunger and the stationary powder. We found that in this condition only about 10% reaction can be achieved after 5 min of EDAMM. However, if both the plunger and the base vibrate, full reaction is achieved within 5 min. This means that the effectiveness of EDAMM is strongly dependent on powder movement during milling. This represents a significant improvement in our

understanding of the parameters that promote high reaction rates during EDAMM. Although, the reactions occurring during EDAMM are poorly understood, we may say that the primary steps operative during this form of processing are production of the plasma by ionization, and its interaction with powder particles, which themselves are continuously altered by conventional milling processes. Primary ions of a carrier gas (Argon) are produced, which then transfer excitation and ionization to powder particle surfaces, producing ions and radicals – the reactant precursors. The plasma flow of gas ions, free radicals and reactant ions bombard the powder surfaces with high energy causing ion implantation. The interaction between the particle surface and the arriving radicals leads to the nucleation and growth of new phases by deep penetration of ions and subsequent diffusion. These can form agglomerates under the influence of electrostatic forces, and these agglomerates are seen in the SEM micrographs. The localized heating also results in the crystallite size of the reaction products being much larger than those formed by conventional milling.

4. Conclusions

XRD, SEM and EDS and X-ray mapping results demonstrated that Cu₂S can be reduced to pure copper by EDAMM, using either Mg as the reducing agent, and partially reduced to and Cu₂S + Cu₅FeS₄ using Fe as the reducing agent. More generally, it is demonstrated that EDAMM can be employed to generate replacement reactions in a matter of minutes, rather than hours or days. Morphological evidence of the existence of deformed and remelted particles was consistent with arguments based on thermodynamic principals, that high local temperatures can be achieved during EDAMM processing. However, SEM observations also suggested that the bulk of reduction reaction occurred via a mechanism involving the formation of agglomerates of small particles that did not exhibit melting. Experiments under impulse plasma mode, both with and without conventional milling applied demonstrated that a critical condition for the reduction reaction to occur is not based on temperature alone, but on how long the particles are processed within the in the gap between the milling rod and the base, under what we interpret to be 'Dusty Plasma' conditions.

It was also found that a critical condition for the reduction reaction to occur is that the particles are processed within the gap between the milling rod and the base, under what may be described as "Dusty Plasma" conditions.

References

- [1] A. Calka and D. Wexler, *Nature* **419** (2002), p. 147. [Full Text via CrossRef](#) | [View Record in Scopus](#) | [Cited By in Scopus \(50\)](#)
- [2] A. Calka and D. Wexler, *Materials Science Forum* **386–388** (2002), p. 125. [Full Text via CrossRef](#) | [View Record in Scopus](#) | [Cited By in Scopus \(6\)](#)
- [3] P. Baláz, L. Takacs, J.Z. Jiang, V. Soika and M. Luxová, *Materials Science Forum* **386–388** (2002), pp. 257–262. [Full Text via CrossRef](#) | [View Record in Scopus](#) | [Cited By in Scopus \(16\)](#)
- [4] P. Matteazzi and G. LeCaër, *Materials Science and Engineering A* **156** (1992), pp. 229–237. [Abstract](#) | [PDF \(636 K\)](#) | [View Record in Scopus](#) | [Cited By in Scopus \(33\)](#)
- [5] J.Z. Jiang, R.K. Larsen, R. Lin, S. Morup, I. Chorkendorff, K. Nielsen, K. Hansen and K. West, *Journal of Solid State Chemistry* **138** (1998), pp. 114–125. [Abstract](#) | [PDF \(755 K\)](#) | [View Record in Scopus](#) | [Cited By in Scopus \(34\)](#)
- [6] G.M. Gusev and V.I. Molchanov, *Proceedings of All-Union Soviet Conference "Mechanochemical Phenomena by Ultrafine Milling*, Academy of Sciences of Soviet Republic, Siberian Branch, Institute of Geology and Geophysics, Novosibirsk (1971), pp. 55–61 (in Russian).
- [7] O. Kubaschewski and C.B. Alcock, *Metallurgical Thermo-chemistry* (5th ed.), Pergamon Press, Oxford, UK (1979) pp. 282–344.
- [8] H.G. Lee, *Chemical Thermodynamics for Metals and Materials*, Imperial College Press, London, UK (1999) p. 277.
- [9] I. Barin, O. Knacke and O. Kubaschewski, *Thermochemical Properties of Inorganic Substances*, Springer-Verlag, Berlin, Germany (1977) pp. 220–251.
- [10] V.E. Fortova, A.V. Ivlevb, S.A. Khrapakb, A.G. Khrapaka and G.E. Morfillb, *Physics Reports* **421** (2005), pp. 1–103.
- [11] Chun Rong, Jizhong Zhang, Chizi Liu and Size Yang, *Phys. Status Solidi (a)* **195** (2) (2003), pp. 375–382. [Full Text via CrossRef](#) | [View Record in Scopus](#) | [Cited By in Scopus \(1\)](#)
- [12] J.D. Gilchrist, *Extraction Metallurgy* (3rd ed.), Pergamon Press, Oxford (1989).



Corresponding author. Tel.: +61 2 42214945; fax: +61 2 42213112.

[Journal of Alloys and Compounds](#)

Volume 486, Issues 1-2, 3 November 2009, Pages 492-496

[Result list](#) | [previous](#) < 106 of 184 > [next](#)

[Home](#)[Browse](#)[Search](#)[My Settings](#)[Alerts](#)[Help](#)

[About ScienceDirect](#) | [Contact Us](#) | [Information for Advertisers](#) | [Terms & Conditions](#) | [Privacy Policy](#)

University of Wollongong



Copyright © 2010 [Elsevier B.V.](#) All rights reserved. ScienceDirect® is a registered trademark of Elsevier B.V.